[20] Timoshenko, S. and Woinowsky-Krieger, S., *Theory of Plates and Shells*, McGraw-Hill, New York, 1959, p. 379.
[21] Lekhnitskii, S. G., "Anisotropic Plates," *Contributions to the Metallurgy of Steel*, No. 50, American Iron and Steel Institute, New York, 1956.
[22] Bogner, F. K., Fox, R. L., and Schmit, L. A., Jr., "The Generation of Interelement-Compatible Stiffness and Mass Matrices by the Use of Interpolation Formulas," *Proceedings of the Conference on Matrix Methods in Structural Mechanics*, Wright-Patterson Air Force Base, Dayton, Ohio, Oct. 1965; also AFFDL-TR-66-80, p. 397.
[23] Isakson, G., Armen, H., Jr., and Pifko, A., "Discrete-Element Methods for the Plastic Analysis of Structures," CR-803, Oct. 1967, NASA.
[24] Timoshenko, S. P. and Gere, J. M., *Theory of Elastic Stability*, McGraw-Hill, New York, 1961.

OCTOBER 1969 AIAA JOURNAL VOL. 7, NO. 10

Static and Dynamic Applications of a High-Precision Triangular Plate Bending Element

G. R. Cowper,* E. Kosko,† G. M. Lindberg,* and M. D. Olson‡
National Aeronautical Establishment, National Research Council of Canada, Ottawa, Canada

A fully conforming plate bending element of arbitrary triangular shape is developed and applied to the solution of several static and dynamic plate problems. The element incorporates 18 generalized coordinates, namely the transverse displacement and its first and second derivatives at each vertex. Example applications presented include static and dynamic analyses of a square plate with edges either simply supported or clamped, statics of an equilateral triangular simply supported plate, and vibrations of cantilevered triangular plates. Rates of convergence of the finite element approximations are investigated both theoretically and numerically. Excellent accuracy is achieved in all cases, and the rates of error convergence agree closely with predicted asymptotic values.

Nomenclature

$\{A\}$	=	column vector of coefficients a_i, Eq. (7)
a,b,c	=	element dimensions, Fig. 1
a_i	=	coefficients of quintic polynomial, Eq. (2)
D	=	plate flexural rigidity = $Et^3/12(1-\nu^2)$
E	=	Young's modulus
$F(m,n)$	=	modified Euler's beta function, Eq. (14)
$[K],[k]$	=	stiffness matrices, Eqs. (12) and (18)
L	=	length of side of square or triangular plate
$[M],[m]$	=	consistent mass matrices, Eqs. (19) and (20)
m_i,n_i	=	exponents of ξ, η in ith term of polynomial, Eq. (2)
N	=	number of elements per side of plate
$\{P\},\{p\}$	=	consistent load vectors, Eqs. (22) and (23)
$[R],[T],$ $[T_1],[T_2]$	=	transformation matrices, Sec. 2
t	=	thickness of plate
$\{W\},\{W_1\}$	=	column vectors of generalized displacements, Eqs. (5) and (16)
w	=	transverse displacement of plate
$w_x,w_{xy},\ldots$	=	$\partial w/\partial x$, $\partial^2 w/\partial x\partial y\ldots$
x,y,ξ,η	=	global and local coordinates, respectively, Fig. 1
θ	=	angle between global and local coordinates, Fig. 1
λ	=	eigenvalue = $\rho t\omega^2 L^4/D$
ν	=	Poisson's ratio
ρ	=	mass density of plate material
ω	=	circular frequency of plate vibration

1.0 Introduction

THE finite element method has proved to be an extremely powerful tool for the analysis of discrete and continuous structures. A good introduction to the subject, which is undergoing rapid and continuing development, can be found in the books by Zienkiewicz[1] and Przemieniecki.[2]

A particularly useful area for the application of finite elements is the static and dynamic analysis of plate bending. Although many finite elements for plate bending have been developed in recent years, only elements of rectangular shape have so far met the requirements of high accuracy and good convergence. The most satisfactory of these is the sixteen degree-of-freedom rectangular element developed by Bogner, Fox, and Schmit,[3] Butlin and Leckie,[4] and later by Mason.[5] Rectangular elements are, however, unsuitable for a great variety of boundary shapes and there is a need for a general triangular element having adequate accuracy and convergence properties.

It is essential for convergence that a finite element be capable of representing a state of uniform strain; in the case of plate bending, this is a state of uniform curvature or uniform twist. Rigid body displacements, which are states of zero strain, should be included among the states of uniform strain. A further desirable property of a plate bending element is conformity. Conformity in this context means that slopes are continuous between elements, as well as transverse displacements. Several convergence proofs are now available for conforming elements, and such elements have the useful property of furnishing lower bounds on the actual strain energy of a plate. Under certain conditions this property can imply monotonic convergence of the strain energy.

Conforming triangular elements for plate bending have been developed by Bazeley et al.[6], and by Clough and Tocher,[7] but these allow only a linear variation of slope normal to an edge and give rather poor results. Suggested improvements to these elements require the introduction of additional nodes on the edges, but this has the inconvenience of making the programing more complicated.

In this paper, the authors present a general triangular element for plate bending that possesses the aforementioned desirable properties. It makes use of six deflection param-

Received January 30, 1969.
* Associate Research Officer, Structures and Materials Laboratory.
† Senior Research Officer.
‡ Assistant Research Officer. Member AIAA.

eters at each vertex, namely the transverse deflection and its first and second derivatives, a total of 18 degrees of freedom per element. The displacement function for the element is taken as a quintic polynomial in x and y. The variation of deflection along any edge is then a quintic polynomial in the edgewise coordinate. The six coefficients of the latter polynomial are uniquely determined by three quantities (deflection, edgewise slope, and edgewise curvature) at each of the terminal vertices. Since the general quintic polynomial in two variables depends on 21 constants, three additional conditions may be satisfied. These stipulate that the variation of slope normal to an edge (called herein the normal slope) be a cubic function of the edgewise coordinate. This cubic is uniquely defined by two quantities, the normal slope and the twist, at each of the two terminal vertices. Thus, continuity of displacement and slopes is assured between two elements that have a common edge.

A preliminary report on the development of the element was given in Ref. 8 where the calculations were limited to a right-angled isosceles element and to static problems. The results, however, were extremely encouraging. In the present paper, the development is extended to cover an element of general triangular shape that is then tested in a comprehensive series of static and dynamic problems.

Since carrying out this work, the authors have found that they were not alone in developing this element. The same element is presented by Butlin and Ford in an internal report[9] that appeared shortly after the authors' preliminary paper.[8] In a note published about the same time, Argyris, et al.[10] mention their TUBA 3 element, which appears to be identical with the authors'. However, no numerical results are given. Other researchers have developed a closely related element with 21 degrees of freedom, the three additional degrees of freedom being the normal slopes at the midpoints of the sides. Such an element has been developed by Argyris, et al.,[10,11] by Bosshard,[12] by Bell,[13] and apparently also by Visser[14] and Irons.[15]

The authors have not been able to examine Ref. 14, and only recently obtained a copy of Ref. 13. It turns out that Bell[13] has actually developed three different models: one with 15 degrees of freedom, one with 18 (which is the same as the one developed herein), as well as the one with 21 degrees of freedom. Bell presents limited static results for most of the problems considered herein and also treats a skewed plate, but does not consider any dynamic problems. His conclusion that the 18-degree-of-freedom element is the superior one is in complete agreement with the authors'.

2.0 Derivation of Element Properties

Due to shortage of space, only a brief outline of the element formulation is given here and the reader is referred to Ref. 16 for complete details.

2.1 Coordinate Systems

The coordinates used are shown in Fig. 1, in which x,y are a system of global coordinates and ξ,η are a system of local coordinates for the particular triangular element under consideration. The vertices of the element are lettered in counterclockwise cyclic order as shown.

The dimensions a, b, and c are given by

$$\begin{aligned} a &= \{(x_2 - x_3)(x_2 - x_1) + (y_2 - y_3)(y_2 - y_1)\}/r \\ b &= \{(x_3 - x_1)(x_2 - x_1) + (y_3 - y_1)(y_2 - y_1)\}/r \\ c &= \{(x_2 - x_1)(y_3 - y_1) - (x_3 - x_1)(y_2 - y_1)\}/r \end{aligned} \quad (1)$$

where

$$r = [(x_2 - x_1)^2 + (y_2 - y_1)^2]^{1/2}$$

2.2 Finite Element Deflection

The deflection $w(\xi,\eta)$ within a triangular element is taken as the quintic polynomial

$$\begin{aligned} w(\xi,\eta) = {} & a_1 + a_2\xi + a_3\eta + a_4\xi^2 + a_5\xi\eta + a_6\eta^2 + \\ & a_7\xi^3 + a_8\xi^2\eta + a_9\xi\eta^2 + a_{10}\eta^3 + a_{11}\xi^4 + \\ & a_{12}\xi^3\eta + a_{13}\xi^2\eta^2 + a_{14}\xi\eta^3 + a_{15}\eta^4 + \\ & a_{16}\xi^5 + a_{17}\xi^3\eta^2 + a_{18}\xi^2\eta^3 + a_{19}\xi\eta^4 + a_{20}\eta^5 \end{aligned} \quad (2)$$

Note that the preceding expression does not contain the term $\xi^4\eta$ and hence immediately satisfies the condition that the normal slope be a cubic function in ξ along the edge $\eta = 0$. The conditions for cubic variation of normal slope along the remaining two edges are somewhat more complicated. In investigating these conditions, it is necessary to consider only the terms of fifth degree in (2) since the lower degree terms satisfy the conditions automatically. It may be shown[16] that the condition for cubic variation of the normal slope along the edge P_1P_3 is

$$\begin{aligned} 5b^4ca_{16} + (3b^2c^3 - 2b^4c)a_{17} + (2bc^4 - 3b^3c^2)a_{18} + \\ (c^5 - 4b^2c^3)a_{19} - 5bc^4a_{20} = 0 \end{aligned} \quad (3)$$

Similarly the condition for cubic variation of the normal slope along the edge P_2P_3 is

$$\begin{aligned} 5a^4ca_{16} + (3a^2c^3 - 2a^4c)a_{17} + (-2ac^4 + 3a^3c^2)a_{18} + \\ (c^5 - 4a^2c^3)a_{19} + 5ac^4a_{20} = 0 \end{aligned} \quad (4)$$

The 18 generalized displacements for the element, which are the deflection and its first and second derivatives at each of the three vertices, may be assembled into a column vecto. $\{W_1\}$ whose transpose is

$$\{W_1\}^T = (w_1\ w_{\xi 1}, w_{\eta 1}, w_{\xi\xi 1}, w_{\xi\eta 1}, w_{\eta\eta 1}, w_2, \ \ldots, \ w_3, \ \ldots) \quad (5)$$

where the subscripts 1, 2, 3, denote the vertices P_1,P_2,P_3, respectively, of the element as shown in Fig. 1. $\{W_1\}$ may be evaluated from (2) as

$$\{W_1\} = [T_1]\{A\} \quad (6)$$

where

$$\{A\}^T = (a_1,a_2,a_3, \ \ldots, \ a_{20}) \quad (7)$$

and $[T_1]$ is an 18×20 matrix. When the 18 relations of (6) are augmented by Eqs. (3) and (4), a set of 20 equations for the coefficients a_i is obtained, and can be written as

$$\begin{Bmatrix} W_1 \\ 0 \\ 0 \end{Bmatrix} = [T]\{A\} \quad (8)$$

The matrix $[T]$ is listed in Table 1.

The determinant of $[T]$ has the value $-64\ (a + b)^{17}c^{20} \times (a^2 + c^2)(b^2 + c^2)$ from which it follows that the determinant vanishes only when the area of the triangular element vanishes. Hence $[T]$ is never singular in any practical situation and can be inverted to give

$$\{A\} = [T]^{-1} \begin{Bmatrix} W_1 \\ 0 \\ 0 \end{Bmatrix} \quad (9)$$

which is equivalent to

$$\{A\} = [T_2]\{W_1\} \quad (10)$$

where the 20×18 matrix $[T_2]$ consists of the first 18 columns of $[T]^{-1}$.

2.3 Stiffness Matrix

The stiffness matrix of an element is obtained by a calculation of strain energy. For classical bending of a uniform iso-

tropic plate, the strain energy of an element is

$$U_e = \tfrac{1}{2}D\iint\{w_{\xi\xi}^2 + w_{\eta\eta}^2 + 2\nu w_{\xi\xi}w_{\eta\eta} + 2(1-\nu)w_{\xi\eta}^2\}d\xi d\eta \quad (11)$$

where D is the flexural rigidity, ν is Poisson's ratio, and the integration is taken over the area of the element. By substituting into (11) from (2) and carrying out the necessary integrations, the strain energy may be expressed as a quadratic form in the a_i, thus,

$$U_e = \tfrac{1}{2}D\{A\}^T[k]\{A\} \quad (12)$$

The following closed form expressions were derived in Ref. 16 for the elements of the matrix $[k]$:

$$\begin{aligned}k_{ij} = {} & m_im_j(m_i-1)(m_j-1)F(m_i+m_j-4,n_i+n_j) + \\ & n_in_j(n_i-1)(n_j-1)F(m_i+m_j,n_i+ \\ & n_j-4) + \{2(1-\nu)m_im_jn_in_j + \\ & \nu m_in_j(m_i-1)(n_j-1) + \nu m_jn_i(m_j- \\ & 1)(n_i-1)\}F(m_i+m_j-2,n_i+n_j-2) \quad (13)\end{aligned}$$

where

$$F(m,n) = c^{n+1}\{a^{m+1} - (-b)^{m+1}\}m!n!/(m+n+2)! \quad (14)$$

and m_i and n_i are the exponents of ξ and η in the ith term of (2). All computations involved in evaluating k_{ij} from (13) can be carried out within the computer once the values of a, b, c, m_i, n_i are furnished.

The transformation from global to local coordinates is merely

$$\{W_1\} = [R]\{W\} \quad (15)$$

where

$$\{W\}^T = (w_1,w_{x1},w_{y1},w_{xx1},w_{xy1},w_{yy1},w_2,\ldots,w_3,\ldots) \quad (16)$$

and the rotation matrix $[R]$ is as listed in Table 2. Combining (10, 12, and 15) yields

$$U_e = \tfrac{1}{2}D\{W\}^T[K]\{W\} \quad (17)$$

where

$$[K] = [R]^T[T_2]^T[k][T_2][R] \quad (18)$$

is the required stiffness matrix for the element in the global coordinate system.

2.4 Consistent Mass Matrix

The consistent mass matrix for an element is established in the same way as the stiffness matrix except that the starting point is the formula for the kinetic energy of an element. The kinetic energy of an element in terms of $\{W\}$ is

$$T_e = \tfrac{1}{2}\omega^2\rho t\{W\}^T[M]\{W\} \quad (19)$$

where $[M]$, the consistent mass matrix relative to the global system is given by

$$[M] = [R]^T[T_2]^T[m][T_2][R] \quad (20)$$

The elements of the matrix $[m]$ are given by

$$m_{ij} = F(m_i+m_j,n_i+n_j) \quad (21)$$

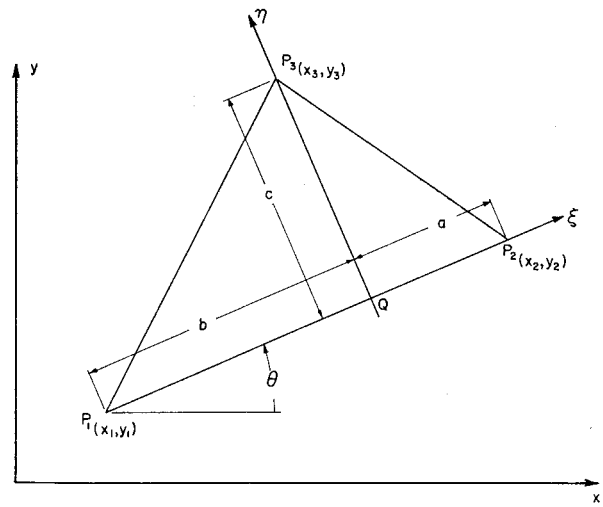

Fig. 1 Coordinate systems.

2.5 Consistent Load Vector

The consistent load vector, established by calculating the virtual work done by the applied load $q(\xi,\eta)$, is

$$\{P\} = [R]^T[T_2]^T\{p\} \quad (22)$$

where the entries in the column vector $\{p\}$ are

$$p_i = \iint q\xi^{m_i}\eta^{n_i}d\xi d\eta \quad (23)$$

Two special cases are considered. The first is a uniform load of intensity q_0 in which case the terms p_i are given by

$$p_i = q_0F(m_i,n_i) \quad (24)$$

The second case is a point load P_0 applied at the point ξ_0, η_0 within the triangle. In this case q is a delta function and it

Table 1 Transformation matrix [T]

1	$-b$	0	b^2	0	0	$-b^3$	0	0	0	b^4	0	0	0	0	$-b^5$	0	0	0	0
0	1	0	$-2b$	0	0	$3b^2$	0	0	0	$-4b^3$	0	0	0	0	$5b^4$	0	0	0	0
0	0	1	0	$-b$	0	0	b^2	0	0	0	$-b^3$	0	0	0	0	0	0	0	0
0	0	0	2	0	0	$-6b$	0	0	0	$12b^2$	0	0	0	0	$-20b^3$	0	0	0	0
0	0	0	0	1	0	0	$-2b$	0	0	0	$3b^2$	0	0	0	0	0	0	0	0
0	0	0	0	0	2	0	0	$-2b$	0	0	0	$2b^2$	0	0	0	$-2b^3$	0	0	0
1	a	0	a^2	0	0	a^3	0	0	0	a^4	0	0	0	0	a^5	0	0	0	0
0	1	0	$2a$	0	0	$3a^2$	0	0	0	$4a^3$	0	0	0	0	$5a^4$	0	0	0	0
0	0	1	0	a	0	0	a^2	0	0	0	a^3	0	0	0	0	0	0	0	0
0	0	0	2	0	0	$6a$	0	0	0	$12a^2$	0	0	0	0	$20a^3$	0	0	0	0
0	0	0	0	1	0	0	$2a$	0	0	0	$3a^2$	0	0	0	0	0	0	0	0
0	0	0	0	0	2	0	0	$2a$	0	0	0	$2a^2$	0	0	0	$2a^3$	0	0	0
1	0	c	0	0	c^2	0	0	0	c^3	0	0	0	0	c^4	0	0	0	0	c^5
0	1	0	0	c	0	0	0	c^2	0	0	0	0	c^3	0	0	0	0	c^4	0
0	0	1	0	0	$2c$	0	0	0	$3c^2$	0	0	0	0	$4c^3$	0	0	0	0	$5c^4$
0	0	0	2	0	0	0	$2c$	0	0	0	0	$2c^2$	0	0	0	0	$2c^3$	0	0
0	0	0	0	1	0	0	0	$2c$	0	0	0	0	$3c^2$	0	0	0	0	$4c^3$	0
0	0	0	0	0	2	0	0	0	$6c$	0	0	0	0	$12c^2$	0	0	0	0	$20c^3$
0	0	0	0	0	0	0	0	0	0	0	0	0	0	0	$5a^4c,3a^2c^3-2a^4c,-2ac^4+3a^3c^2,c^5-4a^2c^3,5ac^4$				
0	0	0	0	0	0	0	0	0	0	0	0	0	0	0	$5b^4c,3b^2c^3-2b^4c,2bc^4-3b^3c^2,c^5-4b^2c^3,-5bc^4$				

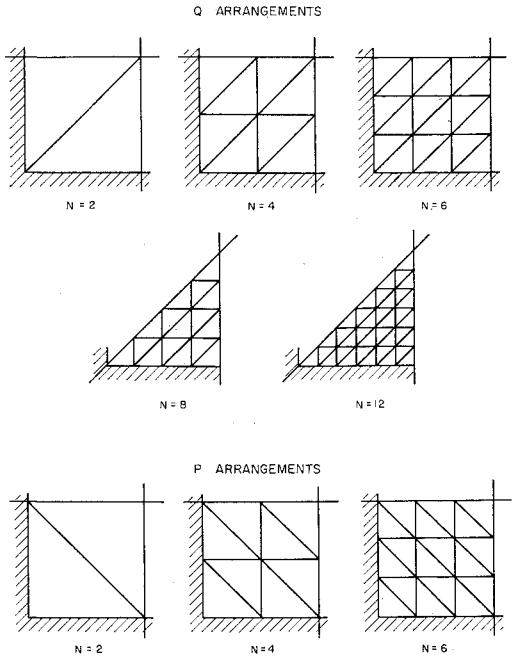

Fig. 2 Layout of finite elements in square plate for static analysis.

follows that

$$p_i = P_0 \xi_0^{m_i} \eta_0^{n_i} \tag{25}$$

2.6 Boundary Conditions

When elements from the class of displacement models are used to solve a problem, it is necessary to satisfy only the kinematic boundary conditions. This is a direct consequence of the theorem of minimum potential energy. The authors have strictly followed this principle, although many writers attempt to satisfy force boundary conditions as well as kinematic ones. For example, Argyris et al.,[11] Bell,[13] and apparently also Butlin and Ford[9] force the normal curvatures (and hence bending moments) to be zero at nodal points on a simply supported boundary. This procedure is of questionable value because it does not guarantee that the normal curvatures will be zero between these nodes. Hence, it merely adds constraints to the finite element system and according to the potential energy theorem can only increase the error. The reader is referred to Ref. 16 for a detailed treatment of the kinematic boundary conditions.

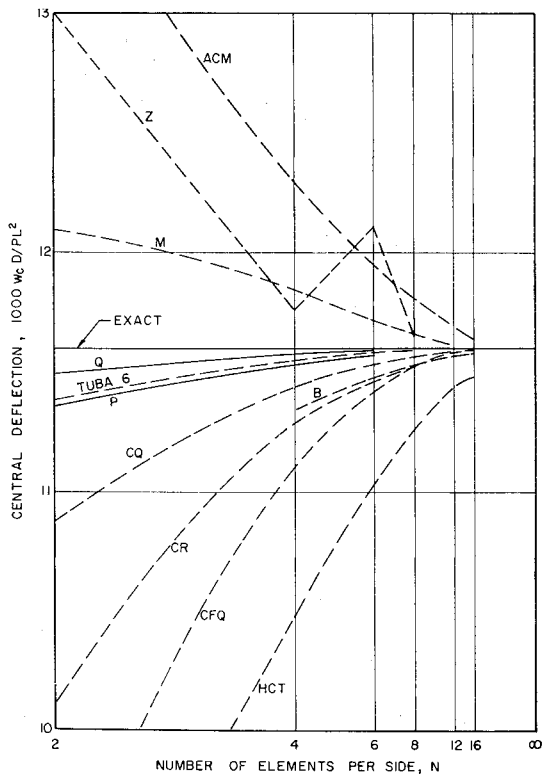

Fig. 3 Simply supported square plate: central deflection under central point load.

Table 2 Rotation matrix [R]

$$[R] = \begin{bmatrix} R_1 & 0 & 0 \\ 0 & R_1 & 0 \\ 0 & 0 & R_1 \end{bmatrix}$$

$$[R_1] = \begin{bmatrix} 1 & 0 & 0 & 0 & 0 & 0 \\ 0 & \cos\theta & \sin\theta & 0 & 0 & 0 \\ 0 & -\sin\theta & \cos\theta & 0 & 0 & 0 \\ 0 & 0 & 0 & \cos^2\theta & 2\sin\theta\cos\theta & \sin^2\theta \\ 0 & 0 & 0 & -\sin\theta\cos\theta & \cos^2\theta - \sin^2\theta & \sin\theta\cos\theta \\ 0 & 0 & 0 & \sin^2\theta & -2\sin\theta\cos\theta & \cos^2\theta \end{bmatrix}$$

3.0 Convergence Properties

In a recent paper by McLay,[17] the notion of order of completeness of conforming finite element deflection functions was introduced. The notion is a useful device for assessing the comparative accuracy of different finite elements, for the higher the order of completeness, the more rapid is the rate of convergence of total strain energy. According to McLay, the finite element displacement function is complete to order n if the error in the quantities that enter into the strain energy is of order h^n, where h is a characteristic dimension of an element.

The displacement function of the present element includes a complete quartic polynomial.§ By Taylor's theorem, a complete quartic polynomial can represent the exact displacement with an error of order h^5. The second derivatives of the displacement, which are the quantities that enter into the strain energy, are represented with an error of order h^3. Hence, in McLay's terminology, the present element is complete to order 3. This is a marked advance beyond the order of accuracy of previously available elements.

It may be shown that the error in strain energy for a static plate problem is then of order h^6 when using the present element, provided the stress field has no singularities. This implies that this error will be asymptotically proportional to N^{-6}, where N is the number of elements per side of the plate. A more detailed and rigorous examination of the element's order of accuracy is given in Ref. 16.

4.0 Numerical Examples

The triangular element is used in the following examples to solve a variety of problems in statics and dynamic of thin isotropic plates. Emphasis is on the accuracy and convergence of the finite element method, and preference is given to cases for which exact solutions are available.

All calculations were carried out on the IBM 360 Model 50 digital computer, using double-precision arithmetic and assuming Poisson's ratio $\nu = 0.3$. As shown in Ref. 16, many of the numerical results are valid for any value of ν.

4.1 Static Analysis of the Square Plate

The various arrangements of the finite elements in a quarter of the square plates are shown in Fig. 2. The number of

§ Recall that the restrictions on normal slopes along element edges constrained the 5th degree terms, so that they were no longer complete.

Table 3 Central deflection and strain energy of simply supported square plate $\nu = 0.3$

Number of elements per side, N	Degrees of freedom for $\frac{1}{4}$ plate	Element arrangement	Central deflection under point load, P $10^2\, w_c\, D/PL^2$	Uniformly distributed load, q_0 Central deflection $10^3\, w_c\, D/q_0L^4$	Uniformly distributed load, q_0 Strain energy $10^4\, UD/q_0^2L^6$
2	8	P	1.1363507	4.0684849	8.4776356
		Q	1.1492790	4.0609374	8.5099612
4	28	P	1.1533253	4.0627265	8.5113962
		Q	1.1574224	4.0623473	8.5124403
6	60	P	1.1570586	4.0623898	8.5124190
		Q	1.1589009	4.0623517	8.5125386
8	63[a]	Q	1.1594190	4.0623524	8.5125496
12	131[a]	Q	1.1597886	4.0623526	8.5125523
Exact solutions			1.1600836	4.0623527	8.5125526

[a] Degrees of freedom for $\frac{1}{4}$ plate.

Table 4 Central deflection and strain energy of clamped square plate $\nu = 0.3$

Number of elements per side, N	Degrees of freedom for $\frac{1}{4}$ plate	Element arrangement	Central deflection under point load, P $10^3 w_c\, D/PL^2$	Uniformly distributed load, q_0 Central deflection $10^3\, w_c\, D/q_0L^4$	Uniformly distributed load, q_0 Strain energy $10^4\, UD/q_0^2L^6$
2	5	P	5.1857973	1.1485043	1.5747418
		Q	5.5346386	1.2612952	1.9243641
4	21	P	5.5427328	1.2643077	1.9351522
		Q	5.5823285	1.2643177	1.9435850
6	49	P	5.5813717	1.2653010	1.9447173
		Q	5.5998956	1.2652304	1.9453183
8	55[a]	Q	5.6053006	1.2652998	1.9455382
12	119[a]	Q	5.6090605	1.2653171	1.9455936
Exact solutions			5.605	1.26	Unknown

[a] Degrees of freedom for $\frac{1}{4}$ plate.

subdivisions of the edge of the square is denoted by N. Symmetry allows the analysis to be limited to one quadrant. For the values $N = 12$ and $N = 16$, advantage was taken also of the symmetry about the diagonal.

4.1.1 Deflections

The calculated values of the deflection at the midpoint of the plate are given in Table 3 for the simply supported plate, and in Table 4 for the clamped plate. These values for the point loaded simply supported plate are compared with results of other finite element approximations in Fig. 3. The code adopted in this diagram follows that of Ref. 7, with some more recent additions. The main characteristics of the various finite elements are listed in Table 5.

The rapid and monotonic convergence of the approximations obtained with the present element, and the small magnitude of the error even for the coarsest grid are apparent from this diagram. In both respects, the "Q" arrangement is superior to the "P" one, and both arrangements are superior to most of the other finite element approximations. Completely analogous results were obtained for the other three cases as well.[16]

In particular, it is interesting to note the results from TUBA 6 (Argyris et al.[11]), which are included in Fig. 3. These results, which are for "P" arrangements, are only marginally better than those from the present element, even though the TUBA 6 element contains three extra degrees of freedom.

It is surprising to see the relatively large error obtained with the element developed by Bosshard (curve B in Fig. 3) who uses the same displacement polynomial as Argyris, et al. The apparent discrepancy may be due to numerical error.

The comparison on the basis of mesh size is obviously unfair to simpler elements that have fewer degrees of freedom per element. It may be argued that a better basis for comparison is the total number of degrees of freedom for a complete problem, as this number gives a measure of the computational effort required. The authors made such a comparison and found that the present element remains far superior to the simpler elements and even becomes slightly superior to the 21-degree-of-freedom element. This somewhat surprising result can be understood by considering the total number of degrees of freedom for a given mesh size. For a complete square plate and specified number N of elements per side, this number is $6N^2 + 12N + 6$ when the present element is used, and $9N^2 + 14N + 6$ when the 21-degree-of-freedom element is used. Hence, the latter element requires up to 50% more degrees of freedom, and yet yields only a marginal increase in accuracy.

4.1.2 Error convergence

The relative errors in the finite element approximations of various relevant quantities are plotted in Figs. 4 and 5 against

Table 5 Comparison of finite element approximations for the bending of a square plate under static loads

Symbol	Type of element[a]	Shape[b]	No. of gen. coordinates per element	Reference
ACM	N	R	12	7
B	C	T	21	12
CFQ	C	Q	19	18
CQ	C	Q	16	19
CR	C	R	16	3, 4, 5
HCT	C	T	9	7
M	N	R	12	20
P,Q	C	T	18	8, 16, and present
TUBA 6	C	T	21	10, 11
Z	N	T	9	6

[a] C = Conforming; N = Nonconforming.
[b] Q = Quadrilateral; R = Rectangular; T = Triangular.

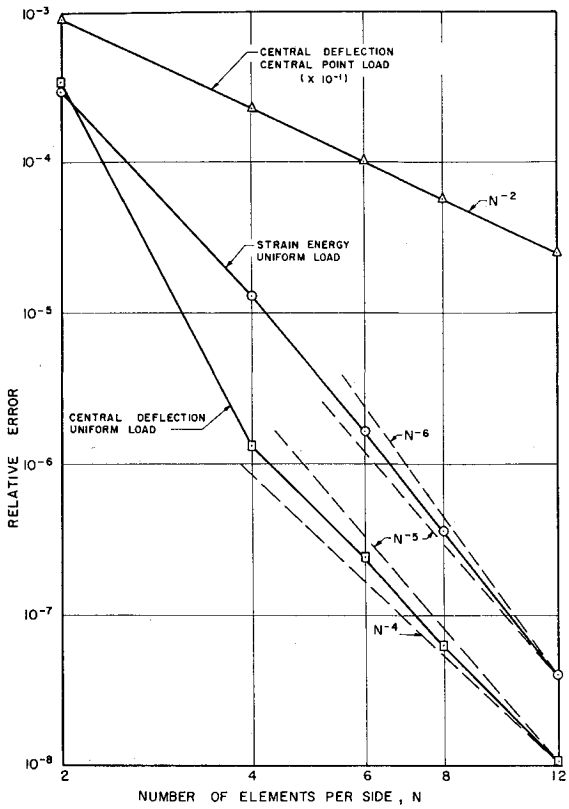

Fig. 4 Simply supported square plate: relative error of finite element solution for "Q" arrangement—central deflection and strain energy.

N, the number of elements per side. Some of the data refer to the central point load case and some to the uniform load case.

For a uniform load case, the theory predicts an error decrement in strain energy proportional to N^{-6}. This prediction is not quite verified, although the results appear to be converging to this asymptotic line. Whether the characteristic exponents will approach the predicted value with a further refinement is purely conjectural and of rather academic interest, since the relative error is smaller than 10^{-7}.

The convergence rates for the other relevant quantities shown in Figs. 4 and 5 are also of interest. Of particular interest is the central bending moment under the uniform load, since it also appears to be converging slowly to the -6 slope. Also, for the uniform load, the asymptotic slopes for the central deflection, midedge bending moment, and corner reaction appear to be -4, -3, and -2, respectively.

The central deflection of the point loaded plate is seen to converge with a slope of -2. Since this deflection is linearly related to the strain energy in this case, this implies that the strain energy also converges with a slope of -2.

Finally, two general comments may be made. One is that the accuracy of the finite element approximation depends in large measure on the arrangement of the elements—for instance, the "P" pattern is consistently inferior to the "Q" pattern, even for a fairly fine mesh. The second is that for cases in which the solutions have singularities as, for example, when concentrated loads are applied, both the accuracy of results and their convergence rate deteriorate appreciably.

4.2 Free Vibrations of the Square Plate

The natural frequencies and corresponding normal modes of a square plate were determined using various "Q" type assemblages of the triangular elements. All the elements are again right isosceles triangles, and N denotes the number of subdivisions of the edge of the square. Two support conditions are considered: simply supported and clamped.

For $N = 4$ and 6, advantage was taken of the symmetry about the nondiagonal axes of the square. The net number of degrees of freedom for each case is listed in Table 6. The headings S-S, S-A, and A-A refer to modes doubly symmetric, symmetric-antisymmetric, and doubly antisymmetric with respect to the nondiagonal axes.

4.2.1 *Numerical results*

Table 7 contains the calculated eigenvalues $\lambda = \rho t\omega^2 L^4/D$ of the simply supported square plate in free vibration. The normal modes of the vibrating plate are classified according to the numbers (r,s) of half waves parallel to the edge directions.

In view of the symmetry of the configuration, one would expect the eigenvalues for (1,2) and (2,1) to be equal. This in fact is exactly the case for all combinations of integers r and s, except for those where the sum $r + s$ (or difference $r - s$) is even. No rigorous explanation can be given for this behavior of the calculated eigenvalues. However, both values appear to converge to the exact solution.

The eigenvectors associated with these not-exactly-equal eigenvalues represent modes in which the nodal lines do not run parallel to the sides, as they should for the simply supported case. For instance, one of the modes that correspond to the (1,3) values has a circular nodal line, whereas in the other mode, the nodal lines coincide with the diagonals. The modes that exhibit this behavior are precisely those for which two nonconfluent eigenvalues are known to exist in the case of clamped edges (see below). For the simply supported plate, a similar behavior of the ($r \pm s$ = even) roots has been observed when using the conforming rectangular finite element of Ref. 3. However, the discrepancy between the two values was much smaller than in the present case. No such discrepancy has been observed in approximations using the 12-degree-of-freedom rectangular elements.

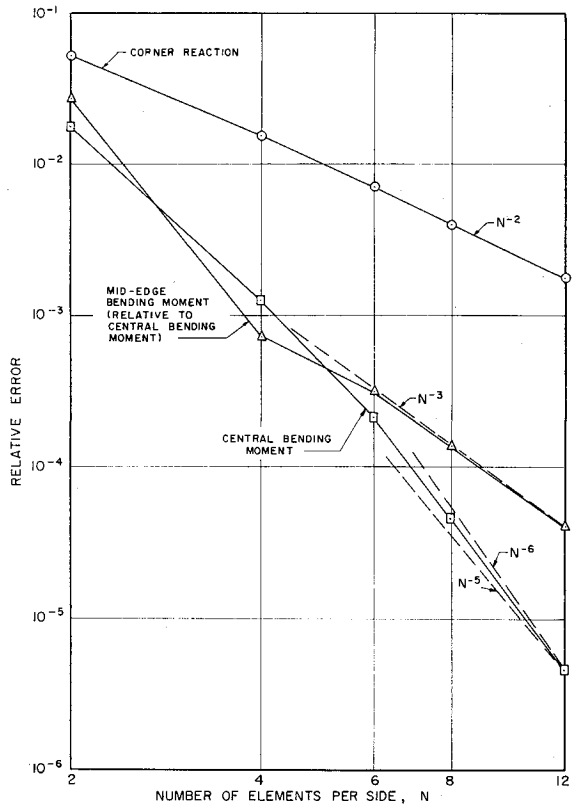

Fig. 5 Simply supported square plate under uniform load: relative error of finite element solution for "Q" arrangement—bending moments and corner reaction.

Table 6 Net degrees of freedom for vibrations of square plate

Edges	$N = 2$	$N = 4$ S-S	$N = 4$ S-A	$N = 4$ A-A	$N = 6$ S-S	$N = 6$ S-A	$N = 6$ A-A
Simply supported	18	28	23	20	60	53	48
Clamped	10	21	16	13	...	...	...

The exact eigenvalues for the simply supported plate are given by

$$\lambda = (r^2 + s^2)^2\pi^4$$

and the lowest 9 values are included in the last column of Table 7. It is seen that the finite element approximations converge monotonically from above to the exact values. The rate of convergence of the relative error is discussed later.

The results of similar calculations for a square plate with clamped edges are summarized in Table 8. Here no exact solution is available, but Ref. 21 contains very close upper and lower bounds for a large number of eigenvalues. The first 10 of these are listed in the last two columns of the table.

Again the finite element approximations converge monotonically from above, but in all cases the approximation with $N = 4$ is still above the upper bound values. The accuracy of the finite element results is not quite as good as in the simply supported case.

For the clamped case, nearly equal roots are expected (see Ref. 22 for example), and indeed do occur in the finite element results. These roots are denoted in the table as $(r,s) \pm (s,r)$. The associated modes of vibration are also correctly predicted by the finite element representations.

4.2.2 Error convergence

The magnitude of the relative error was investigated for the simply supported plate. The plot (Fig. 6) of relative error vs number of elements per side (both scales are logarithmic) shows that the lowest eigenvalue has an error proportional to N^{-6}. The slopes of the error curves for higher eigenvalues appear to be rapidly converging to this value as well. It is interesting to note that within the range of the calculations performed the asymptotic slope is the same as that predicted for potential energy convergence in Sec. 3, namely -6.

4.3 Static Analysis of Equilateral Triangular Plate

This example is chosen to demonstrate the application of the triangular finite element to problems with nonrectangular boundaries. The edges of the plate are assumed to be simply supported and two load cases are considered: a concentrated load applied at the centroid and a uniformly distributed load. For both these cases, analytical solutions are available in Ref. 23.

Table 7 Finite element solutions for eigenvalues λ of simply supported square plate

Mode (r,s)	Number of elements per side, N 2	4	6	Exact solution
(1,1)	389.831	389.63946	389.63663	389.63636
(1,2)	2521.52	2436.37	2435.332	2435.227
(2,2)	6541.94	6238.67	6234.526	6234.182
(1,3)	10152.11	9790.79	9745.30	9740.91
	10083.19	9772.06	9743.64	
(2,3)	20391.4	16553.2	16470.20	16462.14
(1,4)		28505.2	28189.39	28151.23
(3,3)		31748.9	31583.04	31560.55
(2,4)		41252.6	39094.27	38963.64
		39496.5	39028.50	
(3,4)		62741.7	61050.01	60880.68

Table 8 Finite element solutions for eigenvalues λ of clamped square plate

Mode (r,s)	Number of elements per side, N 2	4	Upper bound (Ref. 21)	Lower bound (Ref. 21)
(1,1)	1333.41	1296.06	1294.955	1294.933
(1,2)	5989.70	5411.11	5386.66	5386.42
(2,2)	13609.4	11854.4	11710.83	11709.96
(1,3) − (3,1)	18879.6	17522.8	17313.50	17311.47
(1,3) + (3,1)	19380.1	17630.3	17478.13	17475.96
(2,3)		27867.4	27225.2	27194.9
(1,4)		45409.6	44319.5	44189.1
(3,3)		50414.8	48414.6	48368.8
(2,4) − (4,2)		60891.6	58638.5	58560.3
(2,4) + (4,2)		63962.3	59119.5	59009.7

When the centroid does not fall on a node point, a consistent load matrix is used to represent the point load (see Sec. 2.5). Once the solution is determined, the centroidal deflection is obtained by performing an additional calculation based on the generalized displacements at the three neighboring nodes. The latter calculation is also required in the uniform load case.

The numerical results for centroidal deflections and bending moments and strain energy are presented in Table 9, and relative error plots are given in Fig. 7. It is seen that the strain energy for the uniform load case does converge monotonically as anticipated. The slope of the error curve is approaching -6 for large N, thus confirming the theoretical prediction.

It is apparent that the convergence of the centroidal displacement under the point load (and hence strain energy) is not strictly monotonic as N is varied from 1 to 6. However, if only the consistently refined element arrays $N = 1, 2$, and 4 or $N = 1, 3$, and 6 are considered, the convergence is monotonic. On the other hand, even with this restriction, the centroidal displacement under the uniform load does not converge monotonically. This is not surprising, since the theory pre-

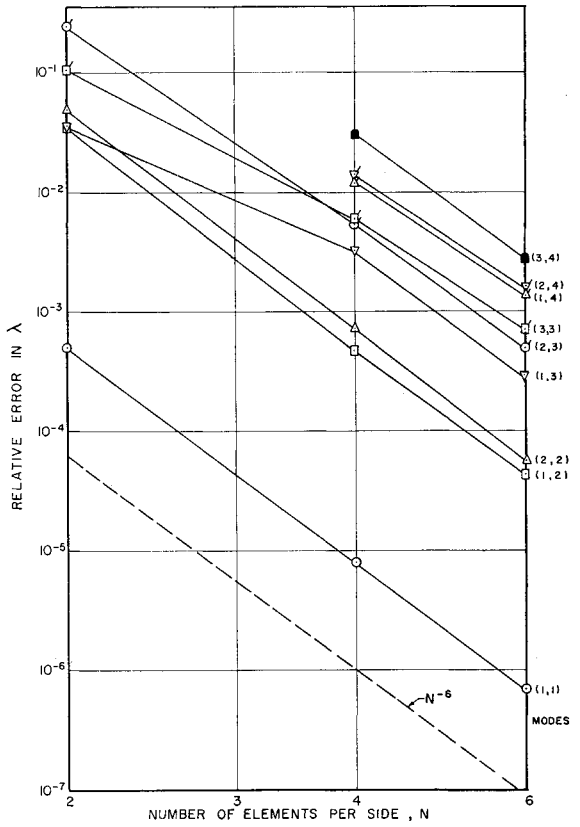

Fig. 6 Simply supported square plate: relative error of finite element solutions for eigenvalues.

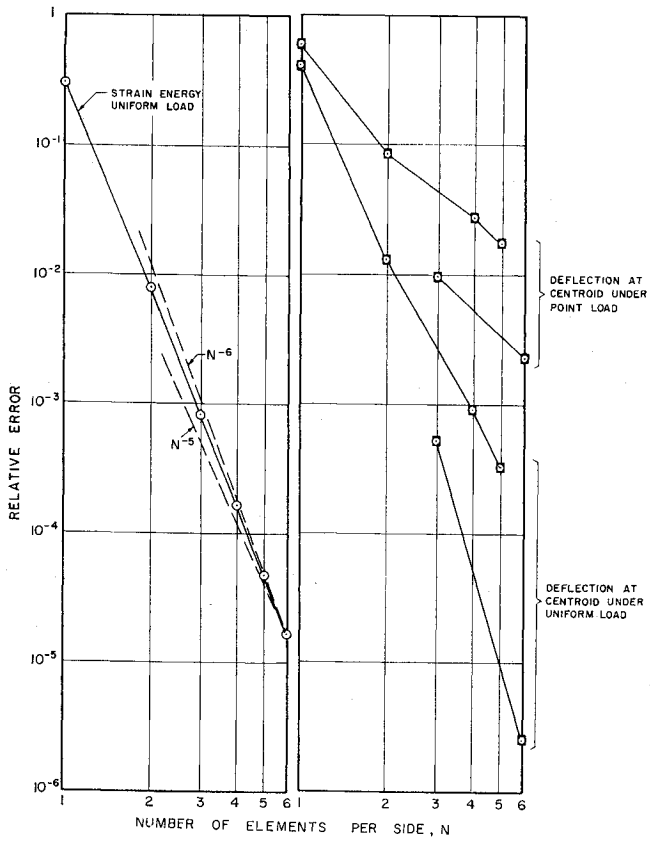

Fig. 7 Simply supported equilateral triangular plate: relative error of finite element solutions.

dicts monotonic convergence only for strain energy. Note that absolute value of the relative error is plotted in Fig. 7 for this case.

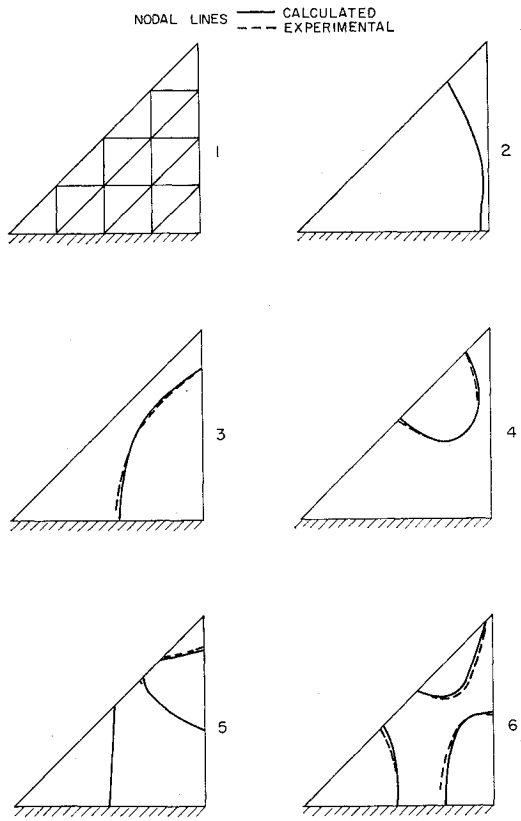

Fig. 8 Cantilever triangular plate, aspect ratio 1: experimental and calculated nodal lines.

Table 9 Finite element solutions for simply supported equilateral triangular plate

NET DEGREES OF FREEDOM	FINITE ELEMENT REPRESENTATIONS	DEFLECTION AT CENTROID UNDER POINT LOAD, P $10^3 w_c D/PL^2$	UNIFORM LOAD, q_o		
			DEFLECTION AT CENTROID $10^4 w_c D/q_o L^4$	STRAIN ENERGY $10^5 UD/q_o^2 L^6$	CENTROIDAL BENDING MOMENT $10^2 M/q_o L^2$
3	N = 1	1.78195	3.4722222	3.382912	0.8125
12	N = 2	3.92237	5.8627658	4.795211	1.907471
27	N = 3	4.24313	5.7840273	4.828753	1.776329
48	N = 4	4.16703	5.7817993	4.831931	1.778990
75	N = 5	4.21168	5.7889363	4.832505	1.820462
108	N = 6	4.27502	5.7870515	4.832651	1.805939
9	A	3.13325	4.9189815	4.322601	1.489583
18	B	4.18775	5.8269240	4.811605	2.076250
18	C	4.06878	5.8490410	4.796294	1.868197
36	D	4.25160	5.7953998	4.824119	1.790700
	EXACT SOLUTIONS	4.28479	5.7870370	4.832731	1.805556

Clearly, the errors in centroidal displacement for the two cases $N = 3$ and $N = 6$, in which the centroid is at a node, do not fit the general trend for either load case. Hence, the points corresponding to these cases are connected by separate lines in Fig. 7. It is seen that these results are significantly more accurate than the others. As pointed out previously, when the centroid is not at a node, special calculation procedures must be introduced. These results indicate that such procedures are less accurate and should be used with caution. No plot is given of the centroidal bending moment for the uniform load case, since the convergence trend is completely analogous to the trend for the centroidal deflection. Note that the relative error is only slightly larger than for the deflection.

The irregular arrangements do not seem to offer any marked advantage when compared to the regular ones. It may be noted that pattern "B" yields a much better approximation than pattern "C," although both patterns contain the same number of elements and have the same number of degrees of freedom. The cause for this difference may be the same as for the difference between the "P" and "Q" arrangements for the square plate. That is, elements having two sides coincident with supported boundaries do not allow as good a representation of the deflections as those that are restrained on one side only.

4.4 Free Vibrations of Cantilevered Triangular Plates

The present section is concerned with plates in the shape of a right triangle having one edge clamped and the other two edges free, similar to fins used for missile stabilization. Vibration experiments on such plates are reported by Gustafson et al.[24]

The first 6 calculated natural frequencies are given for the plate of aspect ratio 1 (45°) in Table 10, along with the available experimental values. Two layouts of finite elements were considered, one with $N = 3$ the other with $N = 4$ subdivisions of the sides of the triangle. Since the difference in the two approximations is not significant, it may be concluded that

Table 10 Natural frequencies of cantilevered triangular plate of aspect ratio 1

MODE NUMBER	FINITE ELEMENT LAYOUTS N=3	FINITE ELEMENT LAYOUTS N=4	EXPERIMENT REF. 24 (H_z)
1	36.6419	36.6201	34.5
2	139.3265	139.2633	136
3	194.1408	194.0186	190
4	333.829	333.433	325
5	455.374	454.197	441
6	593.238	590.514	578

the latter array is sufficiently accurate for practical purposes. The agreement between calculated and experimental frequencies appears to be consistent and very good.

The nodal line patterns associated with the first 6 frequencies are shown in Fig. 8 along with experimental lines (dotted) transferred from photographs in Ref. 24 of Chladni sand figures. Again the agreement between predicted and experimental results is remarkably good. Similar results were obtained for a plate of aspect ratio 0.5.[16]

5.0 Conclusions

A general, conforming triangular plate bending element has been presented and used to solve problems with a wide variety of boundary shapes. The examples presented demonstrate that the element is far superior to those previously available.

The element incorporates a higher order displacement polynomial and more degrees of freedom than most previous elements. The resulting added sophistication gives the element very powerful properties.

Firstly, convergence is assured for all problems, and the rate of convergence is very rapid. The displacement function includes a complete quartic polynomial that implies that in certain static problems the error in strain energy is asymptotically proportional to N^{-6}. This rate of convergence was almost attained in the numerical examples. Rates of convergence of predicted eigenvalues for the simply supported vibrating square plate also approached N^{-6}. Although the rates of convergence of individual displacements or stresses were not examined theoretically, very good answers were obtained in all the examples considered. It was also found that the total number of degrees of freedom required to obtain a desired accuracy was always much smaller when using this element than with lower-order elements.

Another important feature of this element is that unique values of stress are obtained directly at nodal points. The calculated bending moments in the examples were seen to converge rapidly towards the exact values. This element appears to be the first displacement model that adequately predicts stresses.

References

[1] Zienkiewicz, O. C., *The Finite Element Method in Structural and Continuum Mechanics*, McGraw-Hill, London, 1967.

[2] Przemieniecki, J. S., *Theory of Matrix Structural Analysis*, McGraw-Hill, New York, 1968.

[3] Bogner, F. K., Fox, R. L., and Schmit, L. A., Jr., "The Generation of Inter-Element Compatible Stiffness and Mass Matrices by the Use of Interpolation Formulas," (addendum to) *Matrix Methods in Structural Mechanics*, AFFDL-TR-66-80, 1966, Wright-Patterson Air Force Base, Ohio, pp. 397–443.

[4] Butlin, G. A. and Leckie, F. A., "A Study of Finite Elements Applied to Plate Flexure," *Symposium Papers, Numerical Methods for Vibration Problems*, Vol. 3, July 1966, Univ. of Southampton.

[5] Mason, V., "Rectangular Finite Elements for Analysis of Plate Vibrations," *Journal of Sound and Vibration*, Vol. 7, 1968, pp. 437–448.

[6] Bazeley, G. P. et al., "Triangular Elements in Plate Bending—Conforming and Nonconforming Solutions," *Matrix Methods in Structural Mechanics*, AFFDL-TR-66-80, 1966, Wright-Patterson Air Force Base, Ohio, pp. 547–576.

[7] Clough, R. W. and Tocher, J. L., "Finite Element Stiffness Matrices for Analysis of Plate Bending," *Matrix Methods in Structural Mechanics*, AFFDL-TR-66-80, 1966, Wright-Patterson Air Force Base, Ohio, pp. 515–545.

[8] Cowper, G. R. et al., "Formulation of a New Triangular Plate Bending Element," *Transactions of the Canadian Aeronautics and Space Institute*, Vol. 1, 1968, pp. 86–90.

[9] Butlin, G. A. and Ford, R., "A Compatible Triangular Plate Bending Finite Element," Rept. 68-15, Oct. 1968, Engineering Dept., Univ. of Leicester.

[10] Argyris, J. H., Fried, I., and Scharpf, D. W., "The TUBA Family of Plate Elements for the Matrix Displacement Method," *The Aeronautical Journal*, Vol. 72, 1968, pp. 701–709.

[11] Argyris, J. H. et al., "Some New Elements for the Matrix Displacement Method," *Proceedings of the 2nd Conference on Matrix Methods in Structural Mechanics*, Wright-Patterson Air Force Base, Oct. 1968.

[12] Bosshard, W., "Ein neues, vollverträgliches endliches Element für Plattenbiegung," *International Association for Bridge and Structural Engineering Bulletin*, Vol. 28, 1968, pp. 27–40.

[13] Bell, K., "Analysis of Thin Plates in Bending Using Triangular Finite Elements," Feb. 1968, Institutt for Statikk, Norges Tekniske Høgskole, Trondheim.

[14] Visser, W., "The Finite Element Method in Deformation and Heat Conduction Problems," Dr. Ir. dissertation, March 1968, T. H. Delft.

[15] Irons, B. M., "Comments on 'Complete Polynomial Displacement Fields for Finite Elements Method,'" *The Aeronautical Journal*, Vol. 72, 1968, p. 709.

[16] Cowper, G. R. et al., "A High Precision Triangular Plate Bending Element," Aeronautical Rept. LR-514, Dec. 1968, National Research Council of Canada.

[17] McLay, R. W., "Completeness and Convergence Properties of Finite Element Displacement Functions—a General Treatment," AIAA Paper 67-143, New York, 1967.

[18] Clough, R. W. and Felippa, C. A., "A Refined Quadrilateral Element for Analysis of Plate Bending," *Proceedings of the 2nd Conference on Matrix Methods in Structural Mechanics*, Wright-Patterson Air Force Base, Oct. 1968.

[19] de Veubeke, B. F., "A Conforming Finite Element for Plate Bending," *International Journal of Solids and Structures*, Vol. 4, 1968, pp. 95–108.

[20] Melosh, R. J., "A Stiffness Matrix for the Analysis of Thin Plates in Bending," *Journal of the Aerospace Sciences*, Vol. 28, 1961, pp. 34–42.

[21] De Vito, L. et al., "Sul Calcolo dei Autovalori della Piastra Quadrata Incastrata Lungo il Bordo," *Rendiconti dell'Accademia Nazionale dei Lincei*, Ser. 8, Vol. 40, 1966, pp. 725–733.

[22] Warburton, G. B., "The Vibration of Rectangular Plates," *Proceedings of the Institute of Mechanical Engineers*, London, Vol. 168, 1954, pp. 371–381.

[23] Timoshenko, S. and Woinowsky-Krieger, S., *Theory of Plates and Shells*, 2nd ed., McGraw-Hill, New York, 1959.

[24] Gustafson, P. N., Stokey, W. F., and Zorowski, C. F., "An Experimental Study of Natural Vibrations of Cantilevered Triangular Plates," *Journal of the Aeronautical Sciences*, Vol. 20, 1953, pp. 331–337.